

Stationary states of superconducting interferometers with series junctions

S. J. Lewandowski

Instytut Fizyki PAN, Aleja Lotników 32, PL 02-668 Warszawa, Poland

(Received 29 May 1991; revised manuscript received 27 August 1991)

A superconducting interferometer composed of two parallel arrays of series connected Josephson junctions (a simplified model of a high- T_c granular superconductor) is considered. The interferometer is supplied by dc current J from an external source and is linked by an externally applied magnetic flux Φ_e . We consider the associated problems of finding the stationary values of the current in function of Φ_e and stationary values of flux in function of J . It is shown that both problems have identical solutions, which can be obtained by finding the extrema of a properly defined energy function G relative to the conditions given by the set of differential equations $dJ = 0$, $d\Phi_e = 0$, and one of the two conditions found to be complementary, either the fluxoid conservation relationship or the definition of the induced flux Φ_i in terms of currents J_1 and J_2 through the arrays ($J = J_1 + J_2$). The dc Josephson equations and the other of the two "magnetic" constraints are then derived as necessary conditions for the existence of energy extremum, i.e., it suffices that these relations are satisfied only locally at the extremum, a result which can be useful in the investigation of nonequilibrium processes. The stationary values, $G^{(\hat{m})}$, of G are found to depend only on φ_1 and $\varphi_2(\varphi_1)$, the superconducting phase differences across the weakest junction in each array. Functions $G^{(\hat{m})}$ are labeled by different possible phase states $\langle \hat{m} \rangle$ of the system, generated by the numerable set of possible mappings of φ_1 and φ_2 into the phase differences across the other junctions of the system. By allowing the Josephson equations to be satisfied globally, and not only at the extremum, an analytical expression for the second order derivative of $G^{(\hat{m})}$ is obtained. Energy considerations confirm generally unstable and hysteretic behavior of systems containing series junctions.

I. INTRODUCTION

The problem of maximizing dc current J through a parallel arrangement of two series arrays of Josephson junctions linked by an externally applied magnetic flux Φ_e was solved in Ref. 1. Previously such systems received no attention, presumably because no applications could be envisaged for them. However, the advent of high- T_c materials with the well documented (c.f. Ref. 2) existence of intrinsic Josephson junctions has changed the situation. It can be reasonably supposed that some of the intrinsic junctions form series arrays³ and that some of these arrays are connected in parallel. Therefore, the analysis of such systems ceases to be a purely academic exercise and gains in practical significance.

The maximal, or critical, current J_{\max} as a function of Φ_e was found in Ref. 1 to be dependent on the *phase states* $\langle \hat{m} \rangle$ of the system. Roughly, a phase state determines how the superconducting phase difference across the weakest junction in a series array is being mapped, via the Josephson equations, into phase differences across the other junctions of this array. Specifically, it determines whether the cosine of any particular junction phase is positive or negative. Physical significance of the phase states relies on the existence of phase gaps separating the states of individual junctions. The gaps cannot be entered without exceeding the critical current of the weakest junction in the array. In a system containing N junctions in two arrays one must take into account $2(N-2)$ different permutations of the cosine signs (the weakest junctions in each array are disregarded in this respect) and examine $2(N-2)$ different stationary distributions

$J^{(\hat{m})}(\Phi_e)$. Critical current of the system is then defined as $|J_{\max}(\Phi_e)| = \max |J^{(\hat{m})}(\Phi_e)|$, i.e., the envelope of all $J^{(\hat{m})}(\Phi_e)$.

Some aspects of the above analysis are unsatisfactory. It says nothing about the stability of the solutions. The definition of critical current implies that if the system in state $\langle \hat{m} \rangle$ is supplied by a current $J = J_{\max}^{(\hat{m})}(\Phi_e)$, and if a critical current $J_{\max}^{(\hat{m}')}(\Phi_e) > J_{\max}^{(\hat{m})}(\Phi_e)$ is available then an increase of J changes the state to $\langle \hat{m}' \rangle$. However, the existence of phase gaps and associated energy barriers¹ must give certain rigidity in the adherence to the already occupied phase state. It can be supposed that the system in the outlined situation behaves unstably, as it has a choice between going into a resistive state and making the transition $\langle \hat{m} \rangle \rightarrow \langle \hat{m}' \rangle$.

While on the grounds of static theory dynamic behavior of the system cannot be determined, useful hints could be gained by the knowledge of internal energy associated with each phase state. The aim of this paper is to provide this sort of information.

In Sec. II we discuss briefly the previous results, viewing them from a different perspective with particular emphasis put on the initial assumptions. This section serves as a starting point for the development of a more general theory, using a less restrictive and slightly modified set of assumptions, presented in Sec. III. The main result of Sec. III is that the stationary currents $J^{(\hat{m})}(\Phi_e)$ correspond to the stationary values $G^{(\hat{m})}(\Phi_e)$ of a properly defined energy function G . The means to discern between stable and metastable values of $G^{(\hat{m})}(\Phi_e)$ are also provided. Conclusions are presented in Sec. IV.

II. STATIONARY CURRENTS

A. Fundamental relations

We recall that the considered system is a superconducting interferometer composed of two parallel arrays of series connected Josephson junctions. The arrays can also comprise series (lumped) inductances. The interferometer is supplied by dc current J from an external source and is linked by an externally applied magnetic flux Φ_e . A particular realization of such a system, used in numerical examples throughout this paper, is shown in Fig. 1.

The system is best described in terms of superconducting phase differences φ_{ni} across the junctions, where $n = 1, 2$ refers to the array and $i = 1, 2, \dots, N_n$ to the junction in this array. φ_{ni} obey two fundamental relations. The first of these is the set of Josephson equations

$$J_n = I_{ni} \sin \varphi_{ni}, \quad n = 1, 2, \quad i = 1, 2, \dots, N_n, \quad (1)$$

where J_n is the current through an array and I_{ni} is the critical current of a junction in this array. The second is the fluxoid conservation relationship

$$\Phi = (1/2\pi)(\sigma_1 - \sigma_2 + 2\pi q), \quad (2)$$

where Φ is the total flux linking the circuit, expressed in units of flux quantum Φ_0 ($\Phi_0 \cong 2.07 \times 10^{-15}$ Wb), σ_n denotes the sum of all phases in a given array and q is an integer. The phase variables φ_{ni} are related to J directly by Eq. (1) and Kirchoff's law

$$J = J_1 + J_2. \quad (3)$$

Establishing the relationship between φ_{ni} and Φ_e requires some care. Let us define first the *induced* flux Φ_i as the sum of fluxes produced by J_1 and J_2 in series inductances L_1 and L_2 , respectively. Since J_1 and J_2 are in the same direction, their contributions to the flux linking the loop must oppose each other, and we can assume

$$\Phi_i = -J_1 L_1 + J_2 L_2, \quad (4)$$

where L_1 and L_2 are in units of Henry/ Φ_0 .

The relationship between φ_{ni} and Φ_e can be now obtained by expressing the total flux Φ in Eq. (2) as the sum of Φ_e and Φ_i . However, the signs of σ_n in Eq. (2) (determined by the orientation of the fluxoid integration path with respect to J_n) and the arbitrarily chosen signs of J_n in Eq. (4) must be made consistent. At this stage we cannot be certain what is the correct form and we will write

$$\Phi = \Phi_e \pm \Phi_i. \quad (5)$$

This issue will be settled in Sec. III. Meanwhile we note only that in Ref. 1, following other references (c.f. Refs. 4 and 5), the + sign was assumed.

An important consequence of Eqs. (1) – (4) is that the phases φ_{ni} determine not only the currents in the system and the total flux Φ but also — what seems to be less generally recognized — the external flux Φ_e . Conversely, it can be shown that specifying J and Φ_e determines,

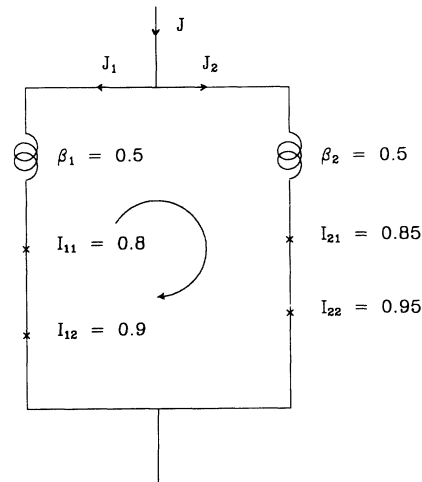


FIG. 1. Schematic representation of a (2+2)-junction interferometer. The junctions are marked by crosses and the indicated values of parameters are used in the numerical example discussed in the text. The arrow in the center indicates the direction of fluxoid integration path.

albeit, in general, not uniquely, the φ_{ni} variables. This can be considered as a manifestation of the more general rule that current and magnetic field in a Josephson junction, if specified together with the superconducting phase difference, must be self-consistent.⁶ Therefore, in order to keep the applied flux constant and equal to Φ_e , while the system is described in terms of φ_{ni} , we must impose formally the constraint

$$\Phi_e = (1/2\pi)(\sigma_1 - \sigma_2) \pm (L_1 J_1 - L_2 J_2) + q = \text{const.} \quad (6)$$

In further considerations of this section, Eq. (6) will effectively replace Eqs. (2), (4), and (5).

B. Solutions

Equations (1) are clearly redundant and the number of independent variables φ_{ni} can be reduced to two. Let us order the indices ni so that $I_{ni} \leq I_{nj}$ for $i < j$ and let us assume $I_{11} \leq I_{21}$. The indices $n1$ will be further abbreviated to n in anticipation of the special role the weakest junction in each array is going to play. We introduce also the notation $a = I_1/I_2$, $a_{ni} = I_n/I_{ni}$. Then Eqs. (1) for $n = 1, 2$ and $i \geq 2$ are rewritten as

$$\varphi_{ni} \equiv \varphi_{ni}^{(m)} = (-1)^{m_{ni}} \varphi_{ni}^{(0)} + m_{ni} \pi, \quad i \geq 2, \quad (7)$$

where m_{ni} is an integer and $\varphi_{ni}^{(0)}$ denotes the principal branch of $\arcsin(a_{ni} \sin \varphi_n)$, i.e., $-\pi/2 \leq \varphi_{ni}^{(0)} \leq \pi/2$. Observe that for $a_{ni} < 1$, the ranges of $\varphi_{ni}^{(m)}$ and $\varphi_{ni}^{(m+1)}$ are separated by a phase gap.

The system is now completely described by the phase differences φ_1 and φ_2 across the weakest junction in each array and by the "state vector" $\langle \hat{m} \rangle = \langle \hat{m}_1, \hat{m}_2 \rangle$ with $N_1 + N_2 - 2$ components $\langle \hat{m} \rangle_{ni} = m_{ni}$. Moreover, the

remaining two equations (1) and Eq. (3) relate φ_1 and φ_2 to each other. Choosing φ_1 , the phase of the weakest junction of the system, as the independent variable, we find that stationary currents must satisfy

$$\frac{dJ}{d\varphi_1} = \frac{\partial J_1}{\partial \varphi_1} + \frac{\partial J_2}{\partial \varphi_2} \varphi_2' \Big|_{\text{extr}} = 0.$$

By using Eq. (1) and differentiating also Eq. (6) (observe that from this instant we are no longer referring to any particular value of Φ_e) φ_2' can be eliminated. After taking into account Eq. (7), the necessary condition for the existence of a current extremum at a phase point (φ_1, φ_2) is obtained in this manner,¹

$$\frac{1}{\cos \varphi_1} + \beta_1^{(\hat{m})}(\varphi_1) = -a \left(\frac{1}{\cos \varphi_2} + \beta_2^{(\hat{m})}(\varphi_2) \right), \quad (8)$$

where

$$\beta_n^{(\hat{m})}(\varphi_n) = \pm \beta_n + \sum_{i=2}^{N_n} \frac{(-1)^{m_{ni}} a_{ni}}{\sqrt{1 - a_{ni}^2 \sin^2 \varphi_n}},$$

and $\beta_n = 2\pi L_n I_n$.

It is evident from the outlined procedure that Eq. (8) can be equally well considered as the necessary condition for the existence of external flux extremum at the same phase point.

Equation (8) must be solved numerically for $\varphi_2^{(\hat{m})}(\varphi_1)$ [or $\varphi_1^{(\hat{m})}(\varphi_2)$], the locus of the stationary points (φ_1, φ_2) , which is dependent on the state vector $\langle \hat{m} \rangle$ assigned to the system. It is impractical, if not impossible, to solve this equation only for some predetermined value of Φ_e or J .

In general, the solution does not exist for an arbitrary value of φ_1 or φ_2 . This can be easily shown in the case of a two-junction interferometer. Then $\beta_n^{(\hat{m})} = \pm \beta_n$ and designating $\alpha = \pm \beta_1 \pm a\beta_2$ it is seen that Eq. (8) is represented by a straight line in $x = (\cos \varphi_1)^{-1}$ and $y = (\cos \varphi_2)^{-1}$ coordinates

$$x + ay + \alpha = 0,$$

everywhere except inside the region bound by the lines $|x| = 1$ and $|y| = 1$. The importance of the parameter α in the analysis of a two-junction interferometer was first realized by Fulton, Dunkleberger, and Dynes.⁷ Intersection points of the solution line with the region boundaries define the forbidden ranges of φ_1 and φ_2 , which are void only for $a = 1$ and $\beta_1 = \beta_2 = 0$. In the general case of nonlinear $\beta_n^{(\hat{m})}$ the straight solution line is replaced by a curve, but the overall picture remains the same, as is demonstrated in Fig. 2 for the particular case of the system shown in Fig. 1.

From the above observations it can be deduced that the plots $\varphi_2^{(\hat{m})}(\varphi_1)$ form on the (φ_1, φ_2) plane closed, periodically spaced loops (in direct analogy to fluxon vortices), separated by regions where stationary solutions cannot exist. The existence of such loops or phase vortices was recognized in the two-junction case by Tsang and Van Duzer.⁵ As a consequence, the plots of $J^{(\hat{m})}(\Phi_e)$ form also closed contours (of width $\geq \Phi_0$), repeated every

Φ_0 , as dictated by the fluxoid conservation.⁸ The gaps in these contours, found in Ref. 1, were due to an imperfect algorithm which failed in regions where the slope φ_2' approached infinity.

The appearance of forbidden gaps in the ranges of stationary phases $\varphi_n^{(\hat{m})}$ is not related to the gaps in φ_{ni} , introduced by Eq. (7). The latter, however, must become wider in the stationary case as a result of the former.

Another important property of Eq. (8) is its invariance under a transformation, which changes simultaneously the sign of $\beta_{1,2}$ and the signs of all $\cos \varphi_{ni}$, including $\cos \varphi_n$. It means that changing the sign in Eq. (5) is equivalent to the inversion of Φ_e [as a consequence of the transformation imposed on the range and domain of $\varphi_2^{(\hat{m})}(\varphi_1)$] and a change in state designation. The latter property might be expressed as

$$\langle \hat{m} \rangle_+ = \langle \hat{m} - 1 \rangle_-, \quad (9)$$

where the subscripts refer to the sign in Eq. (5).

III. EQUILIBRIUM STATES

A. Analytical results

Let us clarify the results of the preceding section. It is evident that in the search for stationary values of the current at fixed external flux, i.e., looking for the solution of the problem $dJ = 0$, $\Phi_e = \text{const}$, we have found also stationary values of external flux at fixed current, i.e., solved the problem $J = \text{const}$, $d\Phi_e = 0$. There is nothing surprising in this observation and it has nothing to do with physics. It is a matter of simple verification that if x_0, y_0 is a stationary point of $f(x, y)$ subject to the constraint $H(x, y, \lambda) = h(x, y) - \lambda = 0$, where λ is a parameter, and if the corresponding stationary value is $f(x_0, y_0) = \xi$, then x_0, y_0 is also a stationary point of $h(x, y)$ relative to the condition $F(x, y, \xi) = f(x, y) - \xi = 0$ and $h(x_0, y_0) = \lambda$. If the method of implicit differentiation, the same which was used in Sec. II B, is employed to solve the problems involving f and h , the link between them is established by the relation $y' = -f'_x/f'_y = -h'_x/h'_y$. It follows that whether the goal is to find a single stationary value of f or h at some specified value of the parameter appearing in the constraint or to obtain the locus of these values, the solution is determined by the set of first-order differential equations

$$df = 0, \quad dh = 0.$$

Keeping in mind the above remarks, we will abandon now the assumptions made in the preceding section and consider a more general problem of minimizing the internal energy of the system under constraints given by

$$dJ = 0, \quad d\Phi_e = 0. \quad (10)$$

This problem may be seen as equivalent to the search for the equilibrium distribution of a given current J into J_1 and J_2 with external flux as a parameter. We assume initially that all phases φ_{ni} are independent. The currents J_n will then depend on all of these variables

$$J_n = J_n(\varphi_{11}, \dots, \varphi_{1N_1}, \varphi_{21}, \dots, \varphi_{2N_2}),$$

and similarly Φ_e , with the reservation that Eq. (10), in general, allows the elimination of one of the φ_{ni} . Since it is not really important at this stage which phase is made dependent, we will denote it by φ^* .

A rather straightforward generalization of expressions valid for less complicated systems (c.f. Refs. 1, 9, and 10), leads to the conclusion that the Gibbs free energy of the system (current source included), scaled by the factor $\Phi_o/2\pi$, is given (in the same units as before) by

$$G = \sum_{ni} I_{ni}(1 - \cos \varphi_{ni}) - \sum_n J_n \sigma_n + (\pi/L)\Phi^2, \quad (11)$$

where $L = L_1 + L_2$.

The first term on the right-hand side of Eq. (11) is the potential energy of the Josephson junctions, the second is the total energy drawn from the current source in the process of increasing the phase across each junction from 0 to φ_{ni} , and the third is the magnetic energy stored in the system (and in the external field).

Equation (11) in the special case $N_1 = N_2 = 1$ must give the Gibbs energy of a two-junction interferometer. Let us observe in this context that the magnetic energy term Φ^2 is sometimes replaced by Φ_i^2 (c.f. Ref. 9). The current source is then required to balance the magnetic energy stored in the system, even if the current drawn from the source is $J = 0$. It can be easily verified that such substitution leads to equilibrium conditions, which have no physical meaning. Obviously, Φ_i^2 can appear in the expression for *free energy* of the system, with the source term dropped.⁴ Correct form of the Gibbs energy for a two-junction interferometer was derived by Klein and Mukherjee.¹⁰

The extrema of G relative to the condition Eq. (10) will occur among those points at which all first order derivatives of G are zero. We must have, therefore,

$$G'_{kj} = \sum_{ni} (I_{ni} \sin \varphi_{ni} - J_n) \varphi_{ni'kj} - \sum_{ni} J_n'_{kj} \varphi_{ni} + (2\pi/L)\Phi \Phi'_{kj} \Big|_{\text{ext}} = 0, \quad (12)$$

where $'kj$ stands for the involved derivative $\frac{\partial}{\partial \varphi_{kj}} + \frac{\partial}{\partial \varphi^*} \frac{\partial \varphi^*}{\partial \varphi_{kj}}$. Since Eq. (12) must occur for all kj , it is clearly seen that the Josephson equations, Eqs. (1), constitute a necessary condition for the existence of the energy extremum. It suffices now that these equations are satisfied locally at the extremum.

Assuming that Eq. (5) is still valid, i.e., $\Phi = \Phi_e \pm \Phi_i$, Eq. (12) on substitution of Eqs. (1) will take the form

$$G'_{kj} \Big|_{\text{ext}} = (-\sigma_1 + \sigma_2) J_{1'kj} \pm (2\pi/L)\Phi \Phi'_{i'kj} = 0, \quad (13)$$

where we have used Eq. (10), in particular the relation $J_{1'kj} + J_{2'kj} = 0$. Incidentally, it is seen from Eq. (13) that if the constraint $d\Phi_e = 0$ is replaced, seemingly in the spirit of fluxoid conservation, by $d\Phi = 0$, then the corresponding relative extremum occurs only at $\Phi = 0$.

To proceed further we need to define Φ as a function of

φ_{ni} , either explicitly as $\Phi(\varphi_{ni})$ or implicitly as $\Phi(J_1, J_2)$. In the first case we have to use the fluxoid conservation relationship Eq. (2), while in the second it is proper to use the induced flux definition Eq. (4). In both cases we will be able to settle the ambiguity in Eq. (5). Let us assume that the fluxoid relationship Eq. (2) is global (differentiable). Equation (13) yields then

$$(\sigma_1 - \sigma_2) [-J_{1'kj} \pm (1/L)\Phi'_{i'kj}] = 0.$$

Clearly, the extremum is either coincident with the minimum of the parabolic magnetic energy term

$$\Phi \propto (\sigma_1 - \sigma_2) = 0,$$

or it is a local extremum, which requires

$$\begin{aligned} (1/2\pi)(\sigma_1 - \sigma_2)'_{kj} \\ = \pm \Phi'_{i'kj} = L J_{1,kj} = (L_1 J_1 - L_2 J_2)'_{kj}. \end{aligned}$$

It is seen immediately that if the lower, minus sign is assumed in the above equation, then — as a consequence of the global fluxoid relationship — the differential form of Eq. (4) will be established as a condition for the existence of energy extremum. We note also the trivial conditions $J_{1'kj} = 0$ and $J_{2'kj} = 0$, corresponding to current expulsion from one of the parallel interferometer arms, i.e., to a situation in which magnetic interaction vanishes (at least within the scope of the present theory).

The complementary character of Eqs. (2) and (4) can be further demonstrated by assuming that it is Eq. (4) which has global character. We have then from Eq. (13)

$$\begin{aligned} (-\sigma_1 + \sigma_2) J_{1'kj} \pm (2\pi/L)\Phi(-L_1 J_{1'kj} + L_2 J_{2,kj}) \\ = (-\sigma_1 + \sigma_2 \mp 2\pi\Phi) J_{1,kj} = 0, \end{aligned}$$

i.e., we obtain Eq. (2) for $q = 0$, again on condition that the lower sign in Eq. (5) is assumed.¹¹ Clearly, the consistency of theory relies on persistent application of this sign.

To conclude, using a less restrictive set of assumptions we have arrived at the same set of fundamental relations, which in the preceding section were shown to determine the stationary values of current and external flux. The solutions of the previous analysis have thus gained a deeper significance as energy extremals. Among the possible applications of these results is the investigation of nonequilibrium processes by the use of multidimensional plots of

$$G(\varphi_{11}, \dots, \varphi_{1N_1}, \varphi_{21}, \dots, \varphi_{2N_2}, J_1, J_2, \Phi_e, \Phi_i)$$

on which the locus of stationary values can be also drawn. For instance, one can easily construct the contour maps of constant energy in the phase space, analogous to the maps for two-junction interferometers.^{9,10}

Judicious "globalization" of the constraints, identified here as local, can be also very useful. Let us assume that the Josephson equations, Eq. (1) and fluxoid, Eq. (2), are global, while the induced flux definition, Eq. (4), is satisfied only at the energy extremum. This corresponds

to a situation in which the superconducting phases adjust immediately to the instantaneous values of J_1 , J_2 , and Φ but these values lag behind the changes in Φ_e . Under these assumptions it is possible¹² to calculate the second derivative $G''(\hat{m})$ of $G(\hat{m})$ with respect to φ_1 , simply by differentiating Eq. (13). After some manipulations we arrive at the result

$$\frac{LG''(\hat{m})}{\cos^2 \varphi_1} = \left(\eta_1^2 \tan \varphi_1 - a^2 \eta_2^2 \tan \varphi_2^{(\hat{m})} \right) \Phi^{(\hat{m})}, \quad (14)$$

where

$$\eta_n^2 = \sum_i \frac{a_{ni}^2}{\cos^2 \varphi_{ni}} = \sum_i \frac{a_{ni}^2}{1 - a_{ni}^2 \sin^2 \varphi_n},$$

and $\Phi^{(\hat{m})}$ denotes the flux calculated from Eqs. (2), (7), and (8). By plotting the sign of this expression along with $J_{\max}(\Phi_e)$ it is possible to indicate the course of the critical current over energy minima, maxima, and inflection points.

B. Numerical example

Since neither Eq. (8) nor Eq. (14) can be solved analytically, further discussion will be limited to the numerical analysis of the already considered example, i.e., the (2+2)-junction interferometer, shown schematically in Fig. 1, where the values of the relevant parameters are also indicated. The (2+2) configuration is the simplest (a state vector with only two components), next to the (2+1) one,⁸ for which the theory of two-junction interferometers ceases to apply. Such configuration was already examined in Ref. 1, but here we have spread more widely the critical currents J_{ni} , getting a more pronounced effect of "spurious modulation" of J_{\max} .

We draw attention to Eq. (9), which is needed to preserve the continuity with the results of Ref. 1, and we keep the subscript "—" in the designation of state vectors as a reminder that total flux Φ is defined here as $\Phi = \Phi_e - \Phi_i$. However, it must be emphasized that Eq. (9) without the accompanying translation of φ_1 and φ_2 is valid only for the current states $J^{(\hat{m})}$ and not for energy states $G^{(\hat{m})}$. The latter are obviously not periodic because of the linear term $\sum \sigma_n J_n$ in Eq. (11).

The inverse cosine plots of Fig. 2 contain several important pieces of information about the stationary properties of the system, which need only to be put into more comprehensive language. Let us remark first that the loops (vortices) of the stationary phase points $\varphi_2^{(\hat{m})}(\varphi_1)$ must by definition form on the φ_1, φ_2 plane a square lattice with lattice constant of 2π . It suffices to consider only a "unit cell" of this lattice with lattice points at $\pm\pi$ and in the center of the resulting square. From the lowest plot in Fig. 2 it is seen that the states with even state vector components m_{ni} occupy the single centered position in the cell. The middle plot shows that states with mixed parity m_{ni} occupy the four corner sites. (Two series junctions in the investigated system signify that two mixed parity states, represented, e.g., by $\langle 0, -1 \rangle_-$

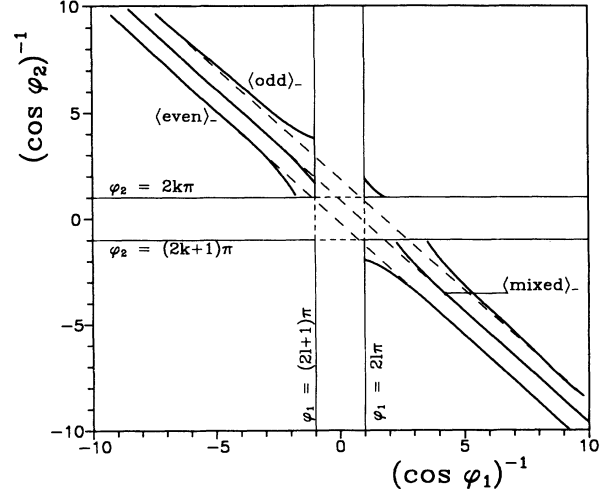


FIG. 2. Plots of inverse cosines of stationary phases for the system shown in Fig. 1, calculated for negative sign of Φ_i in Eq. (5). The lowest plot represents all phase states with m_{ni} even, middle one — the states with mixed parity of m_{ni} , and the upper plot — the states with m_{ni} odd. Dashed lines are to guide the eye only.

and $\langle -1, 0 \rangle_-$ should be considered, but for the assumed values of the system parameters their plots are nearly identical and only one is shown.) Finally, from the upper plot it can be read that states with odd m_{ni} occupy all five sites in the cell. The centered phase vortex is quite small, as indicated by the short central branch of the relevant plot.

The above observations are very helpful in setting up the ranges of φ_1 and φ_2 for computation and in the interpretation of the results. Each phase vortex in a given state produces an identical (modulo Φ_0) current pattern $J^{(\hat{m})}(\Phi_e)$ and, as its unique signature, a distinctive branch of the energy function $G^{(\hat{m})}(\Phi_e)$. Note that moving from one phase vortex to another in the same state involves always a discontinuity in at least one phase φ_n . It can be also shown that only one state representing a given parity of m_{ni} need be considered, the effect of changing the representative being equivalent to the change in φ_1 and φ_2 ranges. Accordingly, we have chosen for further discussion only the states with $m_{ni} = 0, -1$ in the four possible permutations.

In Fig. 3 we show stationary currents and energies for the $\langle 0, 0 \rangle_-$ and $\langle -1, -1 \rangle_-$ states. In order to fit both $J^{(\hat{m})}$ and $G^{(\hat{m})}$ on the same plot so that the correlations between the two could be seen, only negative values of the current less than $I_{\min} = I_2 - I_1$ (normalized to $I_{\max} = I_1 + I_2$) are drawn. Full current plots can be visualized by taking into account their point symmetry with respect to the coordinate origin: $J^{(\hat{m})}(\Phi_e) = -J^{(\hat{m})}(-\Phi_e)$. It was found that the same scale could be used for currents and energies by plotting not directly $G^{(\hat{m})}$, as determined by Eq. (11), but rather $(L/\pi)G^{(\hat{m})}$ with $G^{(\hat{m})}$ normalized also to I_{\max} . The reference level of energy was set equal to $G^{(0,0)}(0)$. The sign of the second-order derivative of energy with respect to φ_1 , calculated from Eq. (14), is indicated by the linewidth used for plotting: thick lines

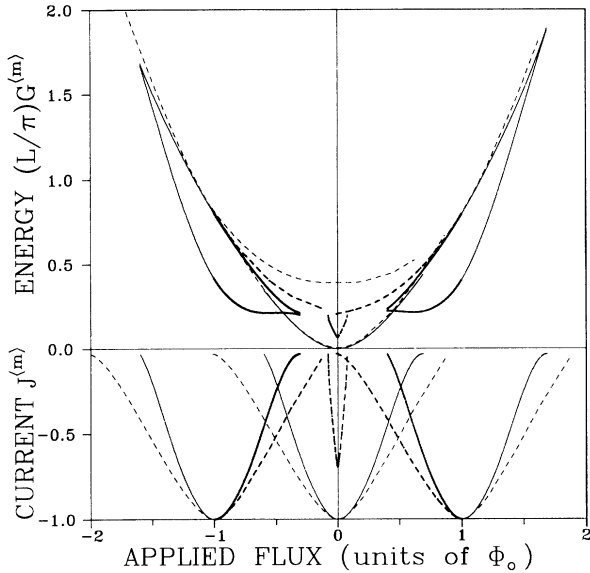


FIG. 3. Stationary energy function $(L/\pi)G^{(\hat{m})}$ (upper part of the drawing) and stationary current $J^{(\hat{m})}$ (lower part of the drawing) in function of externally applied magnetic flux Φ_e for $\langle \hat{m} \rangle = \langle 0, 0 \rangle_-$ (solid lines) and $\langle \hat{m} \rangle = \langle -1, -1 \rangle_-$ (dashed lines) for the system shown in Fig. 1. Both $G^{(\hat{m})}$ and $J^{(\hat{m})}$ are normalized to $I_{\max} = I_1 + I_2$; only negative values of the current are shown. Thick lines are used to draw stable solution branches corresponding to local minima of energy.

correspond to positive sign or local minimum of energy, thin lines – to negative sign or local maximum of energy. The branches drawn with thick lines are supposedly stable and will be referred to by this term.

The $\langle 0, 0 \rangle_-$ plots in Fig. 3 were calculated by allowing φ_1 and φ_2 to take values from the same interval $[-3\pi, 3\pi]$, i.e., by taking into account nine phase vortices arranged in a square. However, the corner vortices to which correspond currents peaking at $\Phi_e = \pm 3\Phi_0$ have very high energies and were omitted from the plots. Currents and energies corresponding to the odd $\langle -1, -1 \rangle_-$ state were calculated by running φ_1 and φ_2 over all five vortices of the unit cell, i.e., by taking the values of these variables from the interval $[-2\pi + \delta, 2\pi - \delta]$, where δ is the half width of the small centered vortex. The contribution of this vortex is clearly seen in Fig. 3 at $\Phi_e = 0$.

A characteristic feature shown in Fig. 3 is the formation of closed energy loops corresponding to vortices, which produce current patterns at identical flux ranges. This effect is particularly well demonstrated for the $\langle 0, 0 \rangle_-$ state, but can be seen also at the central part of the $\langle -1, -1 \rangle_-$ plots. It is also interesting to note that the lowest energy levels of $\langle 0, 0 \rangle_-$ and $\langle -1, -1 \rangle_-$ states are nearly degenerate.

However, the most important conclusion, which can be drawn from Fig. 3, is that the intersection of stationary currents, independently of their state affiliation, in general does not occur at the same Φ_e values as the intersection of corresponding energies.

The limits set for φ_1 and φ_2 in Fig. 3 provide that

vortices of the two states represented there overlap, i.e., both phases can change continuously with Φ_e , on condition that the system changes its state at the appropriate moments. Such continuous phase evolution with applied flux is equivalent to the continuity of stationary currents and leads, after taking into account the other possible phase states, to the critical current of the system defined as the envelope $|J_{\max}(\Phi_e)| = \max |J^{(\hat{m})}(\Phi_e)|$, which was considered in Ref. 1. With the present set of analytical tools we can also consider the system behavior from the point of view of energy continuity and minimization.

The data needed to investigate the system from this point of view are presented in Fig. 4. We have reproduced there from Fig. 3, using the same conventions, the low-energy branches of the $\langle 0, 0 \rangle_-$ state centered at $\Phi_e = \pm\Phi_0$. In addition, we have plotted currents and energies corresponding to $\langle -1, 0 \rangle_-$, $\langle -1, -1 \rangle_-$, lowest energy $\langle 0, 0 \rangle_-$ and $\langle 0, -1 \rangle_-$, the relevant curves being marked *a-a*, *b-b* (dashed), *c-c* and *d-d*, respectively. In order to not clutter the figure with too many details, the latter plots are limited to Φ_e range from approx. $-0.5\Phi_0$ to $0.5\Phi_0$. This range suffices to visualize the critical current envelope, which being Φ_0 periodic can be easily imagined also at the adjoining Φ_e ranges, and encompasses the lowest energy levels of the relevant states. We have omitted also the contribution from the small centered vortex of the $\langle -1, -1 \rangle_-$ state. Comparison with Fig. 3 shows that this contribution, both in current and

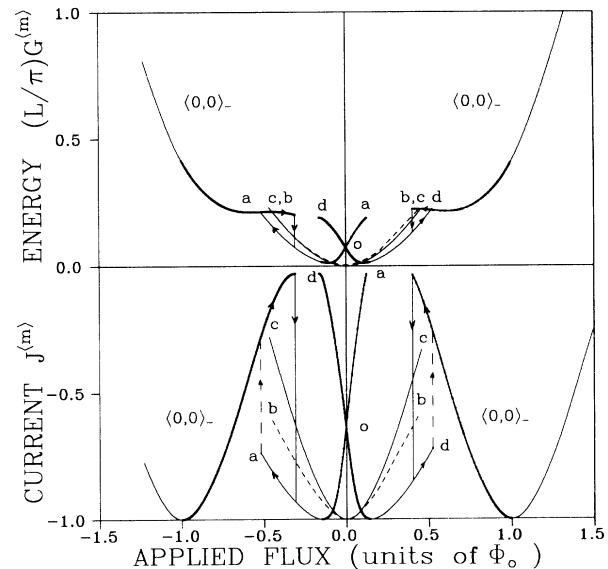


FIG. 4. Possible evolution of critical current and potential energy in function of applied flux Φ_e for the system shown in Fig. 1. Curves marked $\langle 0, 0 \rangle_-$ are reproduced from Fig. 3. The system at $\Phi_e = \pm\Phi_0$ is assumed to be in this state and in the intermediate range has a choice between the states $\langle -1, 0 \rangle_-$ (curves marked *a-a*), $\langle -1, -1 \rangle_-$ (dashed curves *b-b*), central branch of $\langle 0, 0 \rangle_-$ (curves *c-c*), and $\langle 0, -1 \rangle_-$ (curves *d-d*). Stable solutions are drawn with thick lines. Solid vertical lines indicate enforced transitions at a phase vortex limit, dashed lines mark equal energy transitions from an unstable to stable state. Arrows indicate the direction of flux changes.

in energy, is hardly distinguishable from the *d-o-a* composite curves.

Before more detailed discussion let us make two hypothetical rules, which will govern the system's evolution in varying external flux.

(1) When two states have equal stationary energies, the system makes a transition to the state with minimal energy (stable). If both states are stable, the transition is to the state with negative energy slope with respect to flux change.

(2) When the evolution leads beyond a phase vortex limit, the system makes a transition to a state of lower energy.

Let us assume now that at $\Phi_e = -\Phi_0$ the system is in stable $\langle 0, 0 \rangle_-$ state, as shown in Fig. 4, and that Φ_e is increased. The system will stay in the initial state until the phase vortex limit is reached. Application of rule (2) produces then an enforced transition indicated by solid vertical lines on the energy and current plots, and a sudden jump in the current value. For argument's sake we may assume that the transition will be to the state with the lowest energy, i.e., $\langle -1, 0 \rangle_-$ (curves *a-a*). This state will be occupied up to $\Phi_e = 0$, where a transition to the $\langle 0, -1 \rangle_-$ state (curves *d-d*) will take place by rule (1). Finally, with applied flux still increasing, the point of equal energy with the next stable branch of $\langle 0, 0 \rangle_-$ state will be reached and a transition to this state made, producing another sudden jump in the current, as indicated by the dashed vertical line. In this manner we will find the system at $\Phi_e = \Phi_0$ back in the $\langle 0, 0 \rangle_-$ state.

If the applied flux is now decreased to $-\Phi_0$, a similar process will take place, again starting from an "end-of-line" transition marked by solid vertical lines at positive flux values. Clearly a hysteretic loop of current and energy values will be completed between fluxes corresponding to the dashed and solid lines. Similar loops will appear at negative flux values. The picture which emerges from this discussion is that of the system exhibiting mostly currents from below the envelope and only sporadically arriving at the envelope.

Now, our rules are only plausible and cannot be considered as strict. The response of the system to external flux changes must be determined by its dynamic properties. So far, we have carefully abstained from referring to the above-described changes in stationary currents as changes in the critical current of the system. This follows from the conviction that in static theory the current can be always increased, at the expense of potential energy, to the envelope value without driving the system normal. However, the experiments of Fulton, Dunkleberger, and Dynes⁷ on highly inductive two-junction interferometers have put into evidence the phenomenon of multiple critical currents and have shown that in dynamical situations

the equilibrium currents below the envelope can take on the role of critical currents.

Figure 4 demonstrates that such behavior is highly probable for interferometers containing series junctions. The envelope alone shows the effect of "spurious" or "secondary" modulations. The combination of this effect and that of hysteretic multiple critical currents was possibly observed in some high- T_c dc superconducting quantum interference device measurements.¹³ The same combination might be also responsible for the rather poor fit of experimental and theoretical data in experiments on microwave emission from high- T_c thin-films,¹⁴ where only parallel arrays of junctions were used in the theoretical interpretation. Let us also observe that the energy levels in the neighborhood of $\Phi_e = 0$ provide a set of two energy wells required by the two-level fluctuator model of random telegraph noise observed in high- T_c thin films.¹⁵

IV. CONCLUSIONS

In conclusion, we have shown that superconducting interferometers exhibit critical currents, which correspond to the local extrema of the potential energy of the system constituted by the interferometer and its current source, and we have provided the analytical tools which, supplemented by numerical methods, can be used not only to evaluate these currents but also to find whether the corresponding energy extremum is a minimum or a maximum.

The generally unstable and hysteretic behavior of interferometers containing series junctions, already predicted from the analysis of stationary currents,¹ is confirmed by energy considerations. Therefore, the presence of intrinsic series junctions in high- T_c superconductors can be the cause of some of the instabilities observed in these materials. However, the theory presented here is based on a very simplistic model of Josephson junction and it still needs a more definitive experimental verification carried out on classical tunnel junctions.

Finally, let us draw attention to the fact that the theory presented here is composed from the point of view of the weakest junction in the system and it describes, in a manner of speaking, what can be done to the system without driving this junction into the resistive state. In the time-dependent theory a junction in the resistive state can still have ac Josephson properties. Allowing some of the junctions to enter this state might open interesting theoretical and practical possibilities.

ACKNOWLEDGMENT

Many stimulating discussions with J. Zagroziński are gratefully acknowledged.

¹S. J. Lewandowski, Phys. Rev. B **43**, 7776 (1991).

²M. S. Colclough, C. E. Gough, M. Keene, C. M. Muirhead, N. Thomas, J. S. Abell, and S. Sutton, Nature (London) **328**, 47 (1987); G. Jung and J. Konopka, Europhys. Lett.

8, 549 (1989).

³J. Talvacio, M. G. Forrester, and A. I. Braginski, in *Science and Technology of Thin-Film Superconductors*, edited by R. McConnel and S. A. Wolf (Plenum, New York, 1989).

- ⁴K. K. Likharev, *Dynamics of Josephson Junctions and Circuits* (Gordon and Breach, New York, 1988).
- ⁵Won-Tien Tsang and T. Van Duzer, *J. Appl. Phys.* **46**, 4573 (1975).
- ⁶J. Pelka and J. Zagrodziński, *Physica B* **154**, 4573 (1989).
- ⁷T. A. Fulton, L. N. Dunkleberger, and R. C. Dynes, *Phys. Rev. B* **6**, 858 (1972).
- ⁸S. J. Lewandowski, *Acta Phys. Pol.* (to be published).
- ⁹C. D. Tesche, *Physica* **108B**, 1081 (1981).
- ¹⁰M. Klein and A. Mukherjee, *Appl. Phys. Lett.* **40**, 744 (1982).
- ¹¹Full fluxoid conservation relationship could be established by using $\tilde{\Phi} = \Phi - q$, $|\tilde{\Phi}| \leq 1$, instead of Φ in the expression for energy. However, the combination of flux quantum transitions and phase state transitions is difficult to handle.
- ¹²Otherwise it would be not possible to calculate the second derivatives J_n'' .
- ¹³J. C. Gallop, A. J. Marsh, W. J. Radcliffe, and C. D. Langham, in *Proceedings of the European Conference on High- T_c Thin Films and Single Crystals, Ustroń, 1989*, edited by W. Gorzkowski, M. Gutowski, A. Reich, and H. Szymczak (World-Scientific, Singapore, 1990), and references therein.
- ¹⁴G. Jung and J. Konopka, *Europhys. Lett.* **10**, 183 (1989).
- ¹⁵G. Jung, M. Bonaldi, S. Vitale, and J. Konopka, *J. Appl. Phys.* **70**, 5440 (1991).